Thermodynamic and Dynamic Interfacial Properties of Binary Carbon Dioxide−Water Systems

Frédéric Tewes and Frank Boury*

Ingénierie de la Vectorisation Particulaire, INSERM ERIT-M 0104, Bat. IBT,10 rue A. Boquel, 49100 Angers, France

Received: July 22, 2003

We have measured the interfacial tension (γ) between H_2O and CO_2 with a drop tensiometer that permitted us to regulate the drop area and to perform elasticity measurements. We observed that γ decreased with time and with the CO_2 pressure. We first analyzed the adsorption of CO_2 onto surface water by plotting the initial interfacial tension (γ_0) versus CO_2 fugacity and applied Gibbs and then Langmuir-Freundlich equations. We have calculated the interfacial area occupied by CO_2 molecules onto H_2O as well as the equilibrium constant and the thermodynamics parameters of adsorption. This permitted us to understand that the CO_2 was adsorbed onto the surface water by formation of a one-to-one H-type complex with H_2O. Second, we attributed the kinetics phenomena to the formation of interfacial clusters between water and CO_2, which gave interfacial quasi-crystalline structure as shown by compression of the drop area at the end of the adsorption kinetics. We studied this interfacial organization by measuring the apparent elasticity versus time and CO_2 pressure. This measurement allowed us to propose an interfacial organization based on the formation of small blocks, which grow to fill the interface, as already observed by Teng and al.[1] Then we determined the filling of the clusters cavities by analyzing the difference between γ_0 and γ_{eq} ($\Delta\gamma$) by means of the Hill equation. This permitted us to determine that this filling depended on temperature and was cooperative.

1. Introduction

Supercritical CO_2 has many special properties compared to other gases and liquids. For example, its density, compressibility, and dielectric constant are very sensitive to temperature and pressure in the critical region, which is of great interest not only from a fundamental point of view but also for industrial processes.

Like other physical properties, interfacial tension (γ) at the CO_2−water interface is strongly affected by the system properties near the critical point. Interfacial tension plays an important role in the modeling and design of extraction, cleaning, or emulsification processes. For instance, in extraction and cleaning processes, the main factor determining the efficiency of the mass-transfer process is the drop size, which is strongly dependent on interfacial tension, γ between two phases reflects their cohesion and interaction. Therefore, γ between dense CO_2 and water depends on the number and on the energy of interactions between CO_2 and water molecules at the interface and on the organization of this interface. There are specific hydrogen bondings between the oxygen atoms in CO_2 and water molecules,[2,3] which allow water molecules to organize themselves in polyhedral cavities where CO_2 is the guest stabilizing molecule.[1,4−6]

There are few results concerning water−CO_2 interfacial tension measurements. Wilkinson and Chum[7] measured interfacial tension by means of a capillary rise method for CO_2 pressures between 0 and 15 MPa and for different temperatures (5−71 °C). For all temperatures, they found that γ decreased with pressure to an equilibrium value equal to 20 mN/m. They explained the decrease of γ with pressure as a consequence of the increased solubility of CO_2 in the aqueous phase and by the formation of an intermediate third phase at the interface between the CO_{2-} and H_2O-rich phases. In Wilkinson and Chum's work, equilibrium was established very quickly with all systems, in opposition with data from Da Rocha and al.[8] who used a pendant drop tensiometer method and related the decrease of γ with CO_2 pressure and with time.

The goal of this work is to understand the mechanisms that influence the interfacial tension between pressurized CO_2 and water. We will use interfacial rheology and interfacial tension measurement in order to characterize this interface.

2. Materials and Methods

Materials. The vessel was filled with carbon dioxide (purity 0.99) (Air liquide, France). Ultrapure water was produced a by MilliQ plus 188 apparatus (Millipore St Quentin en Yveline, France) and then saturated 12 h with pure CO_2. Tween 40 (Polyoxyethylene (20) Sorbitan Monopalmitate) was purchased by Fluka Chemie, Buchs SG Switzerland.

Pendant Drop Tensiometer. The drop tensiometer (Tracker, IT Concept, Longessaigne, France) allows the determination of the interfacial tension by analyzing the axial symmetric shape (Laplacian profile) of the pendant drop of CO_2-saturated water in pressurized CO_2. The apparatus consisted of a view cell under CO_2 atmosphere, a light source, a CCD camera, a computer, a syringe, and a motor (Figure 1). Pendant drops were formed at the end of a stainless steel tube, 1 mm inside diameter, connected to a syringe. Drop volume and area were controlled during all experiment by a step-by-step motor. Therefore, it was possible to maintain constant the area of the drop during the time of experience, so that the surface tension variation was related only to the adsorption of molecules at the interface.

* Corresponding author. Tel.: +332 41 73 58 68. Fax: +332 41 73 58 03. E-mail: boury@ibt.univ-angers.fr.

10.1021/jp030895c CCC: $27.50
Published on Web 01/22/2004

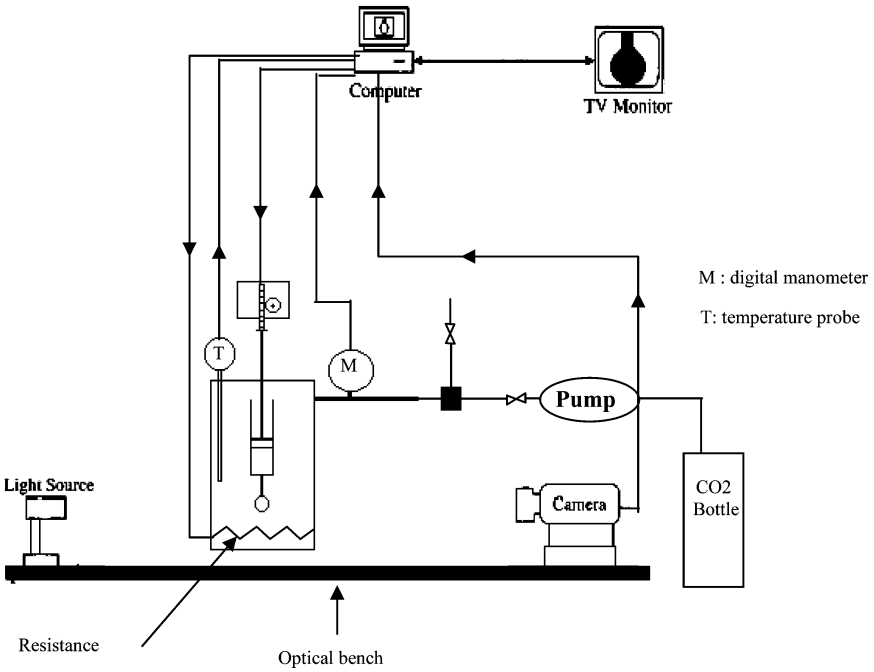

Figure 1. Dynamic drop tensiometer.

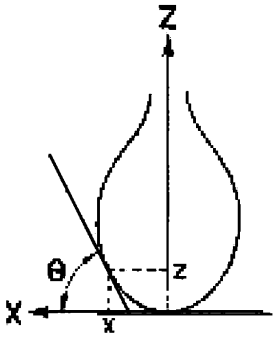

Figure 2. Profile of drop analyzed with Laplace equation.

The interfacial tension was determined by digitizing and analyzing the profile of the droplet (Figure 2) using a CCD camera coupled to a video image profile digitizer board connect to a computer. The drop profile was processed according to the fundamental Laplace equation (eq 1) applied to the drop profile:

$$\frac{1}{x}\frac{\mathrm{d}}{\mathrm{d}x}(x \sin \Theta) = \frac{2}{b} - cz \qquad (1)$$

where x and z are the Cartesian coordinates at any point of the drop profile, b is the radius of the curvature of the drop apex, and θ is the angle of the tangent to the drop profile. In addition, c is the capillarity constant, equal to "$(g\rho)/\gamma$", where ρ is the difference between the densities of the two liquids and g is the acceleration due to gravity. Five times per second, the computer calculates the characteristic parameters of the drop (area, volume, and interfacial tension).

Elasticity Measurement. The common idea of all elasticity measurements is to apply a controlled perturbation to the surface in order to follow simultaneously the related surface pressure variations. We have measured the dynamical response of a surface film (interfacial tension) when a dilational mechanical strain (drop compression) was applied. A slow compression ($1/A_i$) ($\mathrm{d}(\Delta A_t)/\mathrm{d}t$), typically lower than 0.003 s^{-1} was performed in order to reach a total relative strain ($\Delta A(t)/A_i$) of 40−50% of the initial area. From the variation of interfacial tension ($\mathrm{d}\gamma$) versus relative strain, we calculated the interfacial dynamic elasticity as follow:

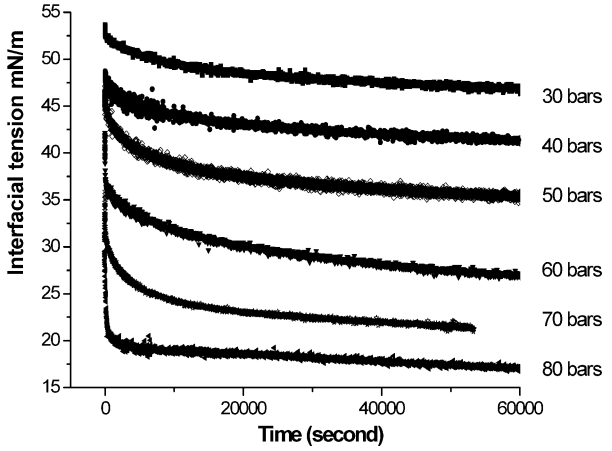

Figure 3. Water/CO_2 interfacial tension versus time for a temperature of 40 °C.

$$E_a = -A_i\frac{\mathrm{d}\gamma}{\mathrm{d}A} \qquad (2)$$

where A_i is the initial drop area and $\mathrm{d}A$ is the deformation.

This dynamic elasticity which is assimilated as an apparent elasticity (E_a), involves the contribution of the elastic properties of the monolayer. It is linked to the number of intermolecular interaction in the interface.

3. Results and Discussion

3.1. Water/CO_2 Interfacial Tension. The water−CO_2 interfacial tensions (γ) versus time have been measured for different pressures (20−90 bar) and temperatures (20, 30. and 40 °C). A typical result obtained at 40 °C is shown in Figure 3. When the data obtained for a same temperature are compared, two processes can be identified. First, γ at time 0 of the kinetics (γ_0) decreased with CO_2 pressure; second, γ between pure water and CO_2 decreased with time for the different tried pressures.

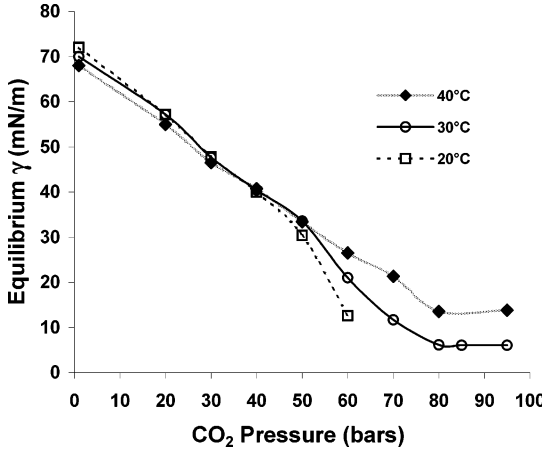

Figure 4. Equilibrium γ at the water/CO_2 interface as a function of CO_2 pressure.

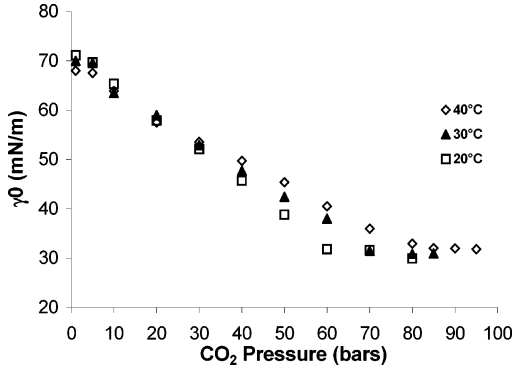

Figure 5. Variation of γ_0 versus CO_2 density.

These results can be separated in two parts. In the first part of the kinetics, γ decreased more intensively and rapidly as CO_2 pressure increased. In the second part, the kinetics slowed and interfacial tension reached an equilibrium value (γ_{eq}) for which the value decreased with pressure.

Comparison of values obtained for a same CO_2 pressure by plotting γ_{eq} versus CO_2 pressure (Figure 4), indicated that after 40 bar, γ_{eq} increased with temperature.

We did not investigated pressures higher than 95 bar because of the characteristics of our apparatus. However, as observed in Figure 4, γ_{eq} remained constant for pressure higher than 80 bar at the different temperatures. This result is in accordance with previous studies,[7,8] which showed that γ between water and pressurized CO_2 reached a stable value in the same range of pressure. Nevertheless, we can remark, that our equilibrium γ values are slightly lower than ones obtained in this studies.[7,8] This can be explained by the longer duration of our experiments (60 000 s).

3.1.1. Variation of γ_0 with CO_2 Pressure. As seen in Figure 5, γ_0 decreased monotonically and intensively until CO_2 pressures comprised between 60 and 80 bar, depending on the temperatures. A constant interfacial tension (31 mN/m) is then obtained for higher pressures, leading for example at 40 °C, to a difference of interfacial tension ($\Delta\gamma_0$) equal to 37 mN/m. This value of 31 mN/m is in accordance with the value calculated from Monte Carlo simulation of the CO_2-water interface at 200 bar and 45.5 °C by Da Rocha and al.[9] (33.2 ± 3.6 mN/m). Their simulation, based on a spatially defined interface of 8 Å, did not included a specific organization of water and CO_2. Therefore, it was related to a simple adsorption of CO_2 onto water.

The processes that occur when we create new CO_2-saturated water drop in the bulk CO_2 can be separated in several steps. In the very first time, CO_2 molecules quickly adsorbed from the bulk CO_2 phase onto the water surface and caused an instantaneous decrease of γ_0. This step is only directed by the CO_2 diffusion if there are not energetic barriers to the adsorption and lead to an equilibration of the CO_2 chemical potential in bulk and at the water surface. This fast phenomenon can be modeled by plotting an isotherm of adsorption Γ versus CO_2 pressure (p_{CO_2}) where Γ is the surface concentration (mol/m^2).

To convert the values of γ_0 into Γ values, we used the Gibbs equation, which describes the equilibrium between the chemical potential of CO_2 into the bulk and the chemical potential of CO_2 adsorbed at the water surface:[10]

$$\Gamma = -\frac{1}{RT}\left[\frac{d\gamma_0}{d\ln p_{CO_2}}\right]_T \quad (3)$$

This equation of state is only valid for low p_{CO_2} since at high pressures, the ideal gas law is not valid and one must take into account fugacity instead of the pressure. Moreover, at the equilibrium, the CO_2 in contact with the water is not pure, but mixed with the water vapor. However, in our pressure and temperature conditions, the solubility of water in CO_2 is low[1] and one can consider only the fugacity for pure CO_2 which is given by

$$f_{CO_2} = p_{CO_2}\exp\left(\frac{B_{(T)}^{CO_2} p_{CO_2}}{RT}\right) \quad (4)$$

where $B_{(T)}^{CO_2}$ is the second virial coefficient for the pure CO_2. This second virial coefficient can be calculated by the expression of Weiss:[11]

$$B_{(T)}^{CO_2} = -1636.75 + 12.0408T - 0.0327957T^2 + 0.00003165T^3 \text{ with } 265\text{ K} < T < 320\text{ K} \quad (5)$$

Expressions 4 and 5 can then be injected into eq 3 to get the γ_0 versus ln f_{CO_2} isotherm (Figure 6a) and to determine the relation between Γ and f_{CO_2} (Figure 6b). This isotherm permitted us to determine the CO_2 molecular area at the saturation state ($A_0 = 1/(\Gamma^\infty \times NA)$).

The adsorption phenomenon can be assimilated to an association chemical reaction in which bulk CO_2 and surface water react to create a new species water$-CO_{2\ surface}$ complex. This phenomenon is governed by an equilibrium constant (eq 6).

$$CO_{2\ bulk} + water_{surface} \rightleftarrows water-CO_{2\ surface} \text{ with } K_d = \frac{f_{CO_2} \times [water]_{surface}}{[water - CO_2]_{surface}} \quad (6)$$

The analysis of the isotherms by a Langmuir-Freundlich or so-called Hill equation (eq 7) allowed us to get the equilibrium constant of dissociation (K_d) of the association−dissociation phenomenon:

$$Y = \frac{\Gamma}{\Gamma^\infty} = \frac{[CO_2]_{surface}}{[CO_2]_{surface\ max}} = \frac{f_{CO_2}^{\ n}}{K_d + f_{CO_2}^{\ n}} \quad (7)$$

where Y is the fractional saturation value and is equal to Γ/Γ^∞. n is the so-called Hill coefficient; this is a measure of the degree of cooperativity of adsorption. In the Langmuir-Freundlich equation, it is a reflection of the fractal dimension of the space

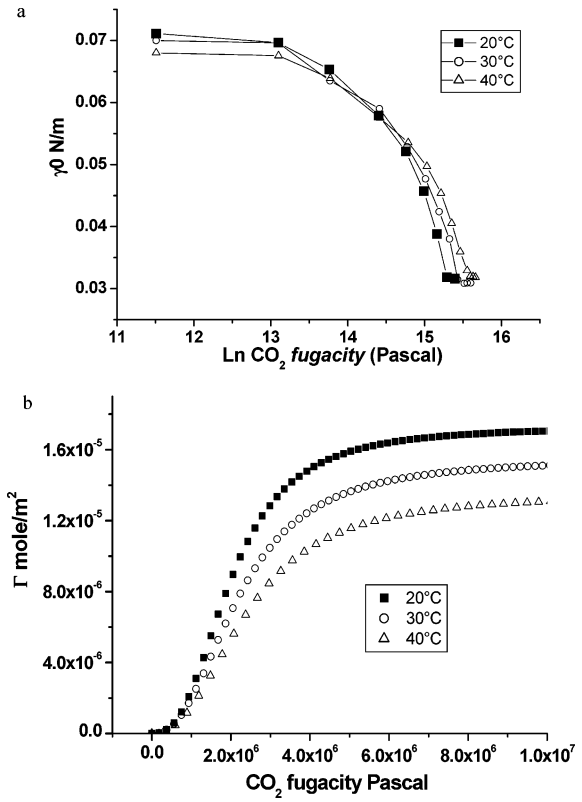

Figure 6. (a) Gibbs representation, (b) isotherm of adsorption.

occupied by the adsorbed molecules. This term relates the deviation from the Langmuir isotherm, which may be attributed to the failure of the assumption of equivalent and independent sites, caused by the intermolecular forces that act between the molecules at the interface. K_d (bars) is the average dissociation constant and is equal to $\sqrt{K_1K_2...K_N}$, where K_1, K_2 are the microscopic dissociation constant of the different step of fixation. It is the $f_{CO_2}{}^n$ that corresponds to the half saturation ($\Gamma^\infty/2$) (deduced from Figure 6b).

To use the Langmuir-Freundlich isotherm, we must assume a maximum monolayer coverage and that the adsorption and desorption rate are equal. We must also make the hypothesis that p_{CO_2} does not change during adsorption. This is supported by the low solubility of CO_2 in water and by the low volume of the water drop (a few microliter) compared to the whole volume of the cell (500 mL) containing the pressurized CO_2.

From the K_d, the standard free Gibbs energy of dissociation can be obtained by using the following equation:

$$\Delta G_T{}^o{}_{\mathrm{dis}} = -RT \ln K_d \tag{8}$$

For condensed phase interactions, the standard enthalpy of adsorption, $\Delta H°$, is derived from the temperature dependence of K_d according to the van't Hoff relation.

$$\Delta H_T{}^{\mathrm{O}}{}_{\mathrm{dis}} = -\mathrm{R}\frac{\mathrm{d}\ln K_d}{\mathrm{d}(1/T)} \tag{9}$$

In addition, the standard entropy is given by

$$\Delta S_T{}^{\mathrm{o}}{}_{\mathrm{dis}} = (\Delta H_T{}^{\mathrm{o}} - \Delta G_T{}^{\mathrm{o}})/T \tag{10}$$

All the data are collected in Table 1. The entropy change for association ($\Delta S_T{}^o{}_{ads} = -48.5$ J/mol·K) in the standard conditions (1 bar) indicates an increase of the molecular order when CO_2 molecules are adsorbed. This decrease in entropy is not compensated by the decrease of the enthalpy. Therefore, the values of $\Delta G_T{}^o{}_{ads}$ show that in the standard conditions (1 bar), the CO_2 adsorption onto water surface is not spontaneous.

The low values of $\Delta H_T{}^o$ show that the CO_2 adsorption is not specific and occurs without any activation barrier. It is characteristic of a physical adsorption or physisorption. This type of adsorption is currently fast and reversible, implying low energy interactions such as electrostatic interactions (hydrogen bond, dipole−dipole interaction, van der Waals attraction), which are the hypotheses we made to use the Langmuir-Freundlich isotherm. The magnitude of the adsorption enthalpies of CO_2 molecules can be related to the number of water molecules complexed with CO_2 molecules and to the cohesion of these complexes. The strength of a hydrogen bond between CO_2 and H_2O depends on the ability of the water surface to act as a hydrogen bond donor and on the induced dipole moment of the carbon dioxide. If we compare our thermodynamical parameters of the adsorption phenomena ($\Delta G_T{}^o$, $\Delta H_T{}^o$, $\Delta S_T{}^o$ at 293 and 303 °K) with the values given for interaction between one CO_2 molecule and one or more water molecules[12] at 298 K, one can remark that our values are very close to the ones corresponding to a single interaction. We can thus conclude that the adsorption of CO_2 molecules onto the water surface lead to a 1/1 complex.

From Γ at saturation, we found the molecular area (A_0) of CO_2 at the maximum of compaction onto the water surface. A_0 (10.9 A^2 at 30 °C) is lower than values found for the CO_2 adsorbed onto solid surfaces made of activated carbon (22.1 A^2 at 28.2 °C)[10] and gives a calculated radius smaller than the van der Waals radius of the CO_2 molecules. This would show that, on the water surface, the CO_2 molecules are more compact than on this solid surface and interact with a different manner. This could be explained by the geometry of the CO_2-H_2O complex formed by electrostatic interaction at the water surface and by the change of charge repartition.

In fact, there are two possible kinds of 1/1 CO_2-H_2O complexes: the T-type and the H-type.[13] In the T-type, the O atom of water faces the C atom and this axis makes an angle of 90° with the OCO axis. In this model, the CO_2 molecules adopt a conformation where the molecules are lying at the water surface with an interfacial area which could be close to the one determined on solid surface. In the H-type, the H atom faces the O atom of CO_2 and the intermolecular C···O axis is tilted off by 10° with the OCO axis (Figure 7).

The low A_0 value found by our measurements could be the results of a low angle between the intermolecular C···O and the OCO axis as is the case with an H-type complex. This hypothesis is also suggested by Monte Carlo simulation of water−CO_2 interface made by Da Rocha et al.,[9] who showed that the formed complexes were made of H-type rather than T-type systems. Therefore, the reduction of A_0, when the temperature decreases, may be due to the increase of the H_{water}···O_{CO_2} interaction and consequently, to the decrease of the angle between the intermolecular C···O axis and the OCO axis. The hypothetical organization of such complex is represented in Figure 7b. It is in accordance with the orientation of water molecules at the water surface, i.e., with the oxygen atoms oriented toward the gas phase.[9,14]

The value of the exponential coefficient of the Langmuir-Freundlich equation, upper to one, indicates that the CO_2 fixation onto water surface is cooperative. The increase of n when temperature is reduced indicates an increase of the cooperativity. This cooperativity can be due to the modification of the water surface by the adsorption of the first CO_2 molecules; which

TABLE 1: Value Calculated from Isotherms Data[a,b]

temperature	Γ^{∞} (mol/m^2)	A_0 (A^2/molecule)	K_d (bars)	$\Delta G_T{}^o{}_{ads}$ (J/mol)	$\Delta H_T{}^o{}_{ads}$ (J/mol.K)	$\Delta S_T{}^o$ads (J/mol.K)	n
293 K	1.72E-05	9.6	19.9	7285	−6938	−48.56	2.63
303 K	1.52E-05	10.9	22.1	7798	−6938	−48.62	2.42
313 K	1.35E-05	12.3	23.9	8260	−6938	−48.56	2.39

[a] The reference pressure of the standard thermodynamical value is 1 bar. [b] $\Delta G_T{}^o{}_{dis} = -\Delta G_T{}^o{}_{ads}$; $\Delta H_T{}^o{}_{dis} = -\Delta H_T{}^o{}_{ads}$; $\Delta S_T{}^o{}_{dis} = -\Delta S_T{}^o{}_{ads}$

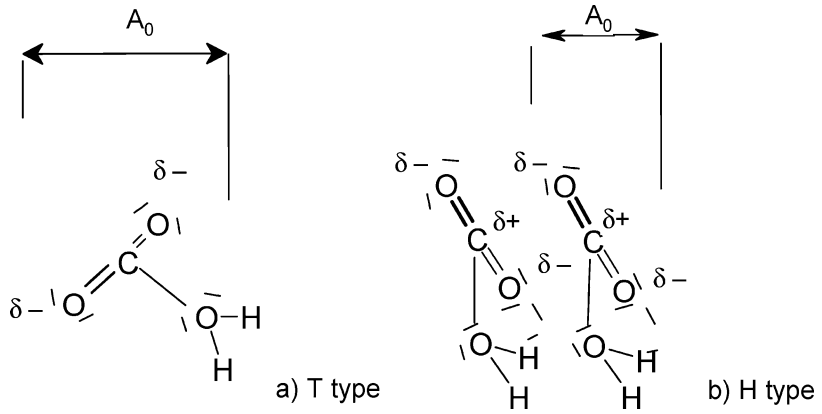

Figure 7. Possible structure of water−CO_2 interaction onto water surface: (a) T-type; (b) H-type. Dotted line corresponds to electrostatic interaction between the CO_2 and H_2O molecule.

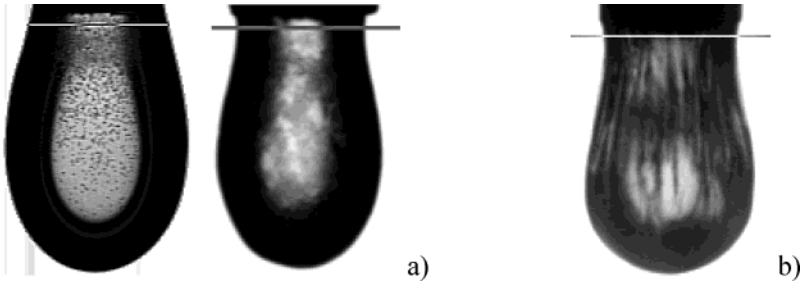

Figure 8. Organization of the water−CO_2 interface (90 bar; 40 °C) by (a) lowering the drop area, (b) cooling the system at the end of the kinetic (time was 50000 s in both a and b experiments).

could exert electrostatic interactions between water molecules and change their organization. This change of water organization would facilitate the fixation of the other CO_2 molecules. Therefore, when the temperature is reduced, the strength of the electrostatic interaction increases and generates an increase of the cooperativity.

3.1.2 Kinetics Effect. Adsorption of CO_2 molecules onto the water surface causes an important decrease of the interfacial tension (γ_0), followed by kinetic effects. This kinetics can be related to an organization of the interface, which leads to an increase of the interaction number or interaction energy between CO_2 and H_2O molecules.

Another phenomenon that indicates such an interfacial structuring is the appearance of a solidlike structure at the end of the kinetics, when the drop area is reduced or when the system is cooled by 2 °C (Figure 8).

After their adsorption onto the water surface, the CO_2 molecules can be transformed into carbonic acid, which is then dissociated into HCO_3^- and H^+. In fact, such dissociation was shown to lead statistically to less than one HCO_3^- ion per 1000 water molecules at 200 bar and 45 °C.[9] Therefore, the kinetic effects cannot be attributed to the adsorption of such ions.

The structure of the interface between water and pressurized CO_2 depends mainly on the characteristics of water. Each water molecule can be linked to four other water molecules through four hydrogen bonds.[3] Therefore, large amounts of water molecules in the liquid state exist in the form of hydrogen-bonded ring structure, i.e., pentagonal and hexagonal rings. These rings are arranged in such a way that they can produce different types of polyhedral cavities, which can be associated to create some clusters.[1,3,15] Such clusters are unstable under their own attractive forces and electrostatic interactions with water molecules in the neighborhood. However, in these clusters, the cavities are large enough to allow some small and nonpolar solute molecules to enter and thus to stabilize the clusters through nonbonding repulsive interactions.[3] CO_2, which is a nonpolar substance with a small molecular diameter, can enter and stabilize this clusters.[1]

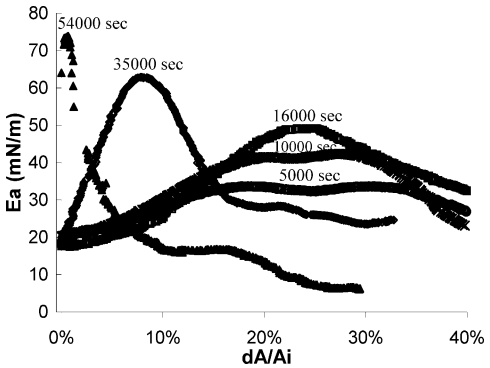

Figure 9. Apparent elasticity versus strain for different time of kinetic at 80 bar.

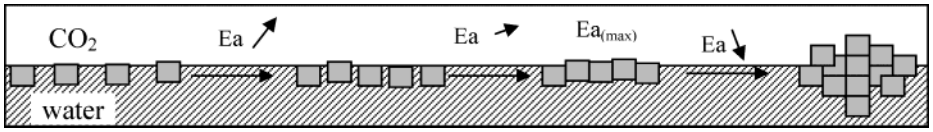

Figure 10. Variation of the interface state during the compression.

At a pressure higher than 45 bar and a temperature less than 10 °C, these clusters, so-called clathrate hydrate or gas hydrate, are in a crystalline state. Above 10 °C, corresponding to our experimental conditions, clusters may be arranged in a quasi-crystalline state, as it was proposed by Teng and al.[1] by interfacial macroscopic observations. This was also shown by Ohgaki and al.[16] by scanning electron microscopy.

Although the CO_2 concentration may be negligible in the bulk water (less than 0.06 mol % at 100 bar and 25 °C),[17] water can be highly supersaturated with CO_2 at the pressurized CO_2−water interface. Due to reorientation of water molecules induced by nonbonding repulsive interactions and supersaturation with CO_2, the interfacial water becomes highly ordered and leads to the formation of clusters. Therefore, this interfacial formation could explain the decrease of γ with time.

To study the formation of those clusters, we first tried to determine their interfacial behavior by measuring the interfacial elasticity versus pCO_2 and versus time. Second, we tried to determine how they are filled and what is the fraction of occupied cages.

3.1.2.1. Interfacial Organization. 3.1.2.1.1. Variation of E_a with Time. Figure 9 shows the variation of $E_a(A_i\, d\pi/dA)$ versus relative interfacial strain (dA/A_i), at different times of the γ kinetic for a CO_2 pressure of 80 bar. Curves had almost a parabolic shape and elasticities versus strain showed a maximum value ($E_{a(max)}$) for a given strain.

This increase of elasticity with the strain could be linked to the increase of the cluster concentration at the interface, caused by the clusters bringing. This bringing leads to the formation of interfacial blocks, as observed on the drop surface in Figure 8a. After the maximal compaction of the interface, giving a $E_{a(max)}$ value, the elasticity decrease could be related to the aggregation and stacking of clusters (Figure 10).

For curves obtained at a pressure of 80 bar, and for short times (5000 to 16000 sec), $E_{a(max)}$ is reached for the same value of strain (0.24), but the peaks become thinner with time. After 16000 s, $E_{a(max)}$ is shift toward lower strain. This shift of $E_{a(max)}$ indicates an increase of the interfacial cluster concentration with time. The more the compression is realized near the equilibrium value the more a low compression is needed to reach the maximal of stacking. At 54000 s, $E_{a(max)}$ is obtained for a very small compression showing a saturation of the interface.

One can also observe that $E_{a(max)}$ increased with time, from 30 mN/m at 5000 s until 75 mN/m at 54000 s for a pressure of 80 bar (Figure 11). This increase of $E_{a(max)}$ with time can be related with the increase of the number or/and of the strength of the molecular interaction and thus an increase of the interactions between clusters, i.e., an augmentation of clusters size.

Finally, since $E_{a(max)}$ increased and is shifted toward low strain more rapidly at 90 bar than at 80 bar, we can conclude that the interfacial clusters concentration increases more quickly when the CO_2 pressure increases. But it seems that $E_{a(max)}$ would reach the same values (Figure 11) for the same strain, indicating that the interface is finally in the same organization state for the two studied pressures. This agrees with the fact that, at equilibrium state, the interfacial tensions were similar for both CO_2 pressures

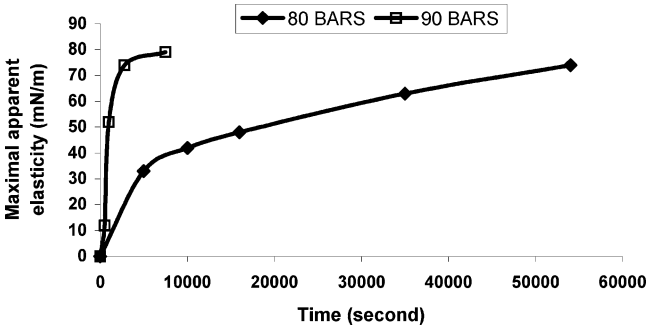

Figure 11. Maximum apparent elasticity versus time of kinetic.

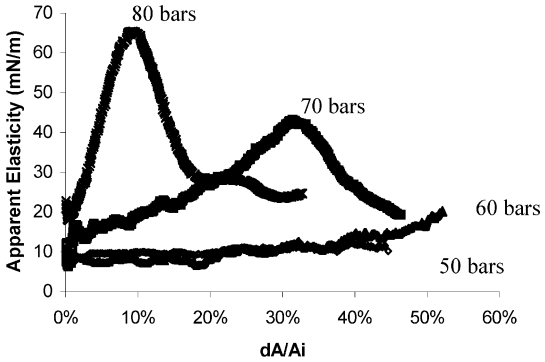

Figure 12. Apparent elasticity versus strain for different pressure at time 35000 s of kinetics.

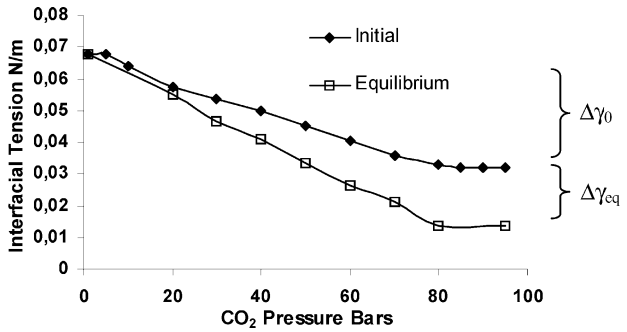

Figure 13. Interfacial tension versus CO_2 pressure at 40 °C: kinetics and initial effect.

3.1.2.1.2. Variation of E_a with CO_2 Pressure. The variations of E_a versus interfacial strain have been measured near the equilibrium state of the kinetics (35 000 s) for different values of the CO_2 pressure (Figure 12).

For pressure less than 60 bar, E_a increased monotonically with the strain. Therefore, below this pressure, the produced strain was not able to aggregate the clusters and to saturate the available interfacial area. For a pressure higher than 70 bar, curves showed a hyperbolic shape. The more the CO_2 pressure was, the more $E_{a(max)}$ was important and obtained with low strain. This shows that equilibrium interfacial concentration of cluster and their degree of organization increased with the CO_2 pressure.

These elasticity measurements are in accordance with the results published by Teng and al.,[1] which showed that at a temperature higher than 10 °C, the interfacial water behaves as

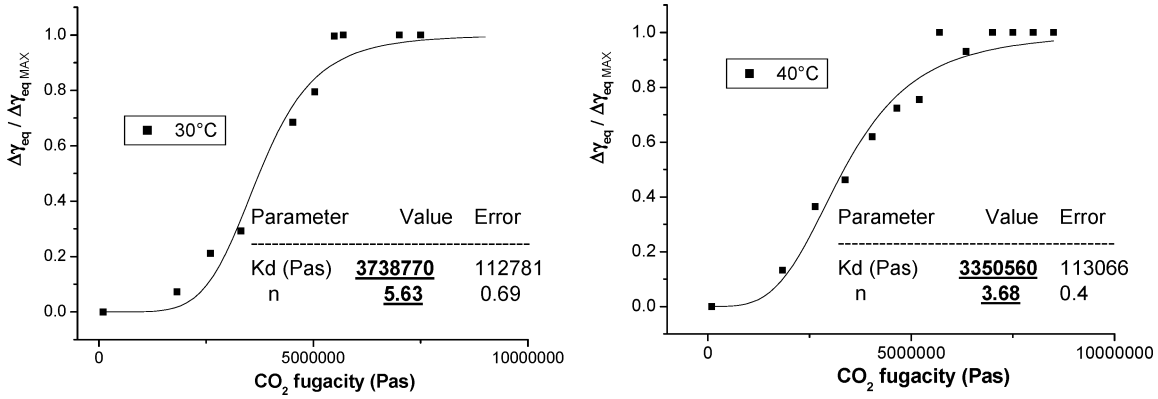

Figure 14. HILL analyses of $\Delta\gamma_{eq}$ by use of Henry law.

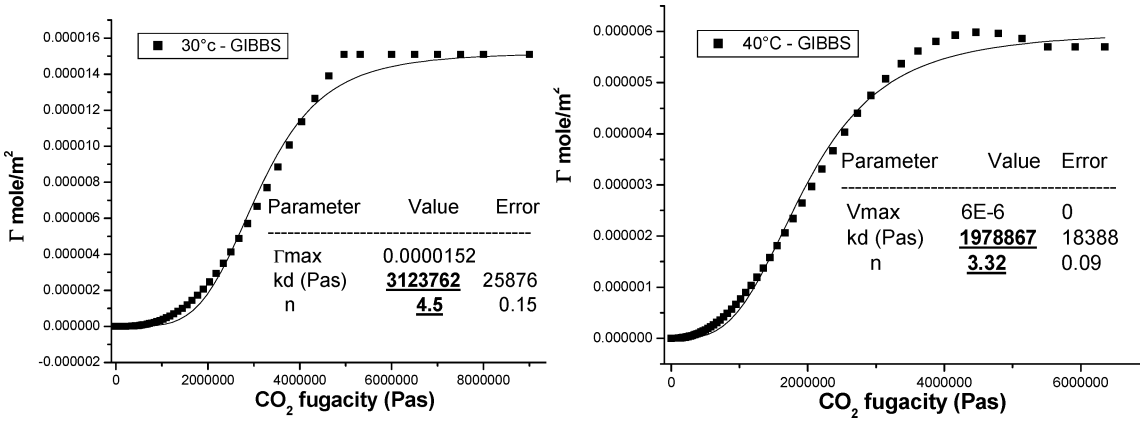

Figure 15. HILL analyses of $\Delta\gamma_{eq}$ by use of Gibbs equation.

an assembly of many small solid pieces. When temperature increases, the water molecules gained energy, which is used to break the hydrogen bonds. Due to the important number of the hydrogen bonds that are involved in the clusters, water molecules at the center of the clusters are able to restore hydrogen bonding after such breakage. In contrast, peripheral molecules will be preferentially lost toward other clusters, or toward less structured environments and interstitial sites. In these conditions, the size of ordered clusters would decrease and the number of smaller clusters would increase, producing the blocks.

3.1.2.2. Filling Determination. In the conditions of clathrate formation, the H_2O-CO_2 clusters are usually made of two types of cavities (small and large). In the hypothesis that in our temperature conditions, the same kind of clusters was created, we want to determine how they are filled and if this process is cooperative (the fixation of the first molecule increases the fixation of the other molecules). For that, we used the Hill equation (eq 7). In this equation, Y is equivalent to the fraction of binding cavities occupied by a ligand, always varying from 0 to 1. n measures the degree of cooperativity, and varies from 1 (no cooperative binding) to N, the total number of bound CO_2 per cluster. As n approaches N, the cooperativity of the system is greater. K_d is the average dissociation constant.

In the theory of the isotherm adsorption, we dealt with surface excess concentration (Γ), whereas experimentally, γ was measured. Before the formation of clusters, there is a spatially defined interface with a very small thickness, composed of a 1/1 CO_2-H_2O complex, giving an interfacial tension equal to γ_0. After the organization of the clusters at the interface, which changes the number and/or the energy of the bond between H_2O and CO_2, the interface is supposed to be less defined (stacked structures) with an interfacial tension equal to γ_{eq} (Figure 13). Therefore, a relation between $\Delta_{\gamma\,eq}$ ($\gamma_0 - \gamma_{eq}$) and Γ is required.

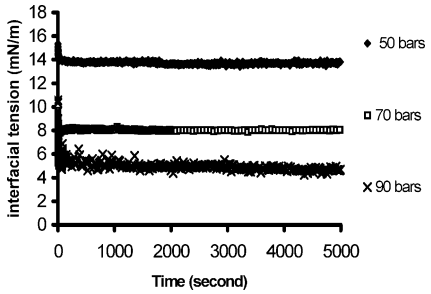

Figure 16. Kinetics of adsorption of Tween 40 (1 g/L) at water−CO_2 interface.

From the different equations describing the adsorption isotherms, we decided to use the simplest Henry equation (eq 11) and the Gibbs equation (eq 3).

$$\Delta\gamma_{eq} = xRT\Gamma \tag{11}$$

In the Henry equation, Γ is proportional to $\Delta\gamma_{eq}$ (eq 11). Thus, in these conditions we can write $Y = \Gamma/\Gamma^{\infty} = \Delta\gamma_{eq}/\Delta\gamma_{eq\,max}$ and plot $\Delta\gamma_{eq}/\Delta\gamma_{eq\,max}$ versus f_{CO_2} (Figure 14) in order to determine the parameters of Hill equation. The use of Gibbs equation allowed us to obtain directly the isotherm (Figure 15).

The Hill coefficient calculated by means of Henry and Gibbs equations shows that the formation of clusters at the water−CO_2 interface, in our experimental conditions, is cooperative. The cooperativity can be explained by the change of water molecules organization, like a change of size cavity, due to the fixation of a first CO_2 molecule. This modification leads to an increase of the affinity between the unfilled cavities and other CO_2 molecules. This is well supported by literature data that suggest that hydrate lattice parameter varies with the guest size.[18]

Therefore, the size of the water cavities changes when the guest molecules enter.

Furthermore, with both equations, n increased when the temperature was reduced. A first possible explanation is the increase of the number of filled cavities. The second explanation is an increase of the cooperativity, without any change of the number of filled cavities. The increase of $\Delta\gamma_{eq}$ and Γ^{∞} when the temperature is reduced shows that the increase of n is mainly due to an increase of the number of filled cavities. Moreover, the augmentation of the average dissociation constant that occurs when the temperature is reduced shows a decrease of the cooperativity. Therefore, at 40 °C, the value of the Hill coefficient, close to 4, led to the supposition that at minimum four cavities are occupied with a CO_2 molecule. The reaction equation of formation of clusters in these conditions can be then written as follows:

$$\text{cluster} + 4CO_2 \leftrightarrow \text{cluster}-((CO_2)_4)$$

At 30 °C, both methods gave almost similar results. The value of n determined with the Henry equation was close to 6 and the one determined by means of the Gibbs equation was close to 5. Consequently, there are at minimum 5 or 6 filled cavities at this temperature. Usually, CO_2 produces clathrates of type I, which are composed of 2 small cavities and 6 large ones.[19] The number of filled cavities that we have found at 30 °C is close to the number of large cavities in this type of hydrate. Thus, we think that under our conditions, such types of clusters are formed with a complete filling of the large cavities.

This type of cluster is composed of 46 water molecules, so we can calculate the hydration number that is defined as the number of water molecules per cluster devided by the number of guest molecules per cluster. Our experimental results lead to values of 11.5 and 7.6 at 40 °C and 30 °C, respectively. The value found at 30 °C is close to the value found by Uchida et al.[20] by Raman spectroscopy at 10 °C and 45 bar.

The variation of filling can also be due to the increase of the cavity size with the temperature as it was shown by Ikeda et al.[21] and Belosludov et al.[18] On raising the temperature, the number of hydrogen bonds decreases and the average distance between the water molecules increases. Therefore, the CO_2 molecules can enter and leave more easily.

3.1.3. Effect of Surfactant Molecules. When short surfactant molecules were added to the system, they quickly adsorbed at the interface and inhibited the time-dependent organization of the water and CO_2 molecules (Figure 11). Therefore, the addition of this type of short surfactant molecules, at this concentration, prevents the formation of this type of cluster, as it was already shown.[22] Consequently, the interfacial pressure of surfactant absorbed at the H_2O-CO_2 interface must be calculated by subtracting the interfacial tension between CO_2 and water at $t = 0$ of the kinetics (not equilibrium values) and the equilibrium tension in the presence of surfactant molecules.

4. Conclusion

The first process that occurs when a water drop is created in CO_2 is the adsorption of CO_2 molecules onto the surface water. This physisorption is responsible for the decrease of γ_0 with the CO_2 pressure and leads to a 1/1 H_2O-CO_2 complex of H-type, as shown from thermodynamics and molecular area values.

After this adsorption, CO_2 molecules diffuse into the water subsurface and then modify their organization. This reorganization of the interface lead, to a time dependent decrease of H_2O-CO_2 interfacial tension until it reaches an equilibrium value. This leads to the formation of H_2O-CO_2 clusters even at temperature higher than the one usually described for the so-called clathrate hydrate formation. In these conditions, elasticity measurement and macroscopic visualization suggest that these clusters are growing by assembly of many small blocks. The interfacial concentration and the size of these blocks increase with time and finally saturation of the interface occurs.

The growth kinetics of this cluster block accelerates with the CO_2 pressure, which is reflected by the acceleration of the decrease of γ with CO_2 pressure in the first part of the γ versus time curves. Therefore, at temperature higher than 10 °C, cluster organization is rather in quasi-crystalline than in crystalline state.

The type of cluster differs also with the temperature. At 40 °C, only four cluster cavities could be filled with a CO_2 molecule, but 6 cavities were estimated to be filled at 30 °C. The analysis of n values strongly suggests that the filling is cooperative. The clusters have all this sterically good cavities filled or empty. This cooperativity could explain that the cluster growth is performed by blocks at the interface.

References and Notes

(1) Teng, H.; Yamasaki, A. *Int. J. Heat Mass Transfer* **1998**, *41*, 3204.
(2) Sato, H.; Matubayasi, N.; Nakahara, M.; Hirata, F. *Chem. Phys. Lett.* **2000**, *323*, 257.
(3) Ludwig, R. *Angew. Chem., Int. Ed.* **2001**, *40*, 1808.
(4) Mori, Y. H. *Energy Convers. Manage*. **1998**, *39*, 1537.
(5) Hagan, M. M. *Clathrate inclusion compounds*; Reinhold: New York, 1962.
(6) Sloan, E. D. *Clathrate hydrates of natural gases*, 2nd, rev. and expanded ed.; Marcel Dekker: New York, Hong Kong, 1998.
(7) Chun, B.-S.; Wilkinson, G. T. *Ind. Eng. Chem. Res.* **1995**, *34*, 4371.
(8) Da Rocha, S. R. P.; Harrison, K. L.; Johnston, K. P. *Langmuir* **1999**, *15*, 419.
(9) Da Rocha, S. R. P.; Johnston, K. P.; Westacott, R. E.; Rossky, P. J. *J. Phys. Chem. B* **2001**, *105*, 12092.
(10) Toth, J. *Adv. Colloid Interface Sci.* **1995**, *55*, 1.
(11) Weiss, R. F. *Mar. Chem.* **1974**, *2*, 203.
(12) Nguyen, M. T.; Raspoet, G.; Vanquickenborne, L. G.; Duijnen, P. T. V. *J. Phys. Chem. A* **1997**, *101*, 7379.
(13) Sadlej, J.; Makarewicz, J.; Chalasinski, G. *J. Chem. Phys.* **1998**, *109*, 3919.
(14) Dukin, S. S.; Kretzschmar, G.; Miller, R. *Dynamics of Adsorption at Liquid Interfaces*; Elsevier: New York, 1995; Vol. 1.
(15) Müller, A.; Reuter, H.; Dillinger, S. *Angew. Chem., Int. Ed.* **1995**, *34*, 2328.
(16) Ohgaki, K.; Kirokawa, N.; Ueda, M. *Chem. Eng. Sci.* **1992**, *47*, 1819.
(17) Mochizuki, M. A. *Energy Convers. Manage.* **1998**, *39*, 567.
(18) Belosludov, V. R.; Inerbaev, T. M.; Subbotin, O. S.; Belosludov, R. V.; Kudoh, J.-i.; Kawazoe, Y. J. *Supramol. Chem*., in press.
(19) Uchida, T. *Waste Manage.* **1997**, *17*, 343.
(20) Uchida, T.; Takagi, A.; Kawabata, J.; Mae, S.; Hondoh, T. *Energy Convers. Manage.* **1995**, *36*, 547.
(21) Ikeda, T.; Yamamuro, O.; Matsuo, T.; Mori, K.; Torii, S.; Kamiyama, T.; Izumi, F.; Ikeda, S.; Mae, S. *J. Phys. Chem. Solids* **1999**, *60*, 1527.
(22) Jakobsen, T.; Sjöblom, J.; Ruoff, P. *Colloids Surf., A* **1996**, *112*, 73.